10th International IFAC Symposium on
Computer Applications in Biotechnology
Preprints Vol.2, June 4-6, 2007, Cancún, Mexico

METABOLIC FLUX ANALYSIS APPLICATIONS TO *ASPERGILLUS NIGER* AB1.13 CULTIVATIONS

G. Melzer[1], A. Dalpiaz[1], Y. Göcke[1], A. Grote[1], M. Kucklick[2], E. Franco-Lara[1], P. Dersch[2], B. Nörtemann[1], D.C. Hempel[1]

1) Institute of Biochemical Engineering,
2) Institute of Microbiology,
Technical University Braunschweig, Germany.

Abstract: A stoichiometric model was developed for *Aspergillus niger* AB1.13. Metabolic flux analysis (MFA) revealed that the pH of the medium does not affect the flux distribution of the central carbon metabolism. However, one exception could be observed regarding the oxaloacetate hydrolase (*OAAH*) reaction. During D-glucose and D-xylose feeding, a 6-fold and 2-fold increase in flux distribution was observed with increasing pH (ΔpH 2.5), respectively. Differences in flux with D-glucose and D-xylose as substrate were reflected in a higher demand of NADPH during D-xylose consumption. Additionally, a comparison between metabolic models revealed that the ribulose-5-phosphate epimerase (*RPE*) might not be expressed during D-xylose consumption.

1. INTRODUCTION

Metabolic Flux Analysis (MFA) is a powerful tool used to quantify the intracellular fluxes from measurements of extra cellular rates, such as substrate and oxygen uptake, carbon dioxide release, product and biomass formation. The method allows the estimation of metabolic flux distributions in living cell systems without considering kinetic behaviour of metabolite transformations by enzymatic activity.
Aspergillus niger is one of the most important filamentous fungi producing a wide variety of organic acids and industrial relevant enzymes. For this reason, the focus of this work was set on the investigation of the metabolic flux distribution considering the main pathways of the central carbon metabolism network and biomass formation of the strain AB1.13. Based on the assumptions of alternative pathways, several modifications of the metabolic network models were performed and assessed. Finally, the influence of the pH and the type of carbon source on the metabolic flux distribution was compared using the proposed metabolic models.

2. MATERIALS AND METHODS

2.1 Strain and medium composition

The filamentous fungus *A. niger* AB1.13 is an uridine auxotrophic, protease deficient and α-glucoamylase producing strain (Mattern et al. 1992) derived from *A. niger* AB4.1 (van Hartingsveldt et al., 1987) by UV-irradiation.
For submerged cultivation, a modified Vogel's medium (Vogel 1956) supplemented with 2 mM uridine was used. The initial concentration of both carbon sources, D-xylose or D-glucose, were adjusted to 67 mM and 56 mM (corresponding to 10 gram per litre for both), respectively.
The medium additionally consisted of 6.6 g/L $(NH_4)_2SO_4$, 2.5 g/L KH_2PO_4, 0.2 g/L $MgSO_4 \cdot 7\ H_2O$, 0.1 g/L $CaCl_2 \cdot 2\ H_2O$ and trace elements (5 mg/L citric acid$\cdot H_2O$, 5mg/L $ZnSO_4 \cdot 7\ H_2O$, 1 mg/L $Fe(NH_4)_2(SO_4)_2 \cdot 6\ H_2O$ 0.16 mg/L $CuSO_4$, 0.05 mg/L H_3BO_3, 0.05 mg/L $Na_2MoO_4 \cdot H_2O$ and 0.037 mg/L $MnSO_4 \cdot H_2O$).

2.2 Chemostat culture conditions

Cultures of *A. niger* AB1.13 were grown in a batch-mode for the first 24 h, which was followed by a continuous cultivation-phase at a working volume of 2.2 litre in a 3 litre Applikon stirred tank bioreactor (Applikon Dependable Instruments, Schiedam, The Netherlands). The feed concentrations of D-glucose and D-xylose were 2 g/L. The cultures were made at a dilution rate of 0.1/h.
The initial inoculum of spores was about 10^6 spores per millilitre of working volume in the bioreactor. The aeration rate and temperature was maintained constant at 0.5 L/L/min and 30°C, respectively.

Cultures using D-xylose or D-glucose as the sole carbon source were made at four different pH values (3, 3.7, 4.7 and 5.5). At each pH the value was kept constantly by the addition of 2M NaOH or 2M HCl. The agitation speed was kept constantly at 550/min using two six-bladed disc turbine impellers. The working volume was maintained at constant level by removing the effluent from the reactor with a peristaltic pump.

2.3 Analytical procedures

Biomass analysis. Cell dry weight was determined by filtration of a sample of constant volume of the fermentation broth using a cellulose acetate filter. Biomass was washed twice with 10 mM sodium-acetate buffer (pH 4.5) and dried for 48 h at 100°C.

HPLC analysis. The quantification of extracellular metabolites was carried out using a HPLC system (Elite Lachrome HITACHI Ltd., Japan) under isocratic conditions. A column (Metacarb 67H, 250 x 4.6 mm, 5 µm), was used with a mobile phase containing 1 mM H_2SO_4 in bi-distilled water at 70°C at a flow rate of 0.8 mL/min. Detection of sugars (glucose, xylose), polyols (mannitol, xylitol) and organic anions (formate, oxalate, acetate, butyrate) was performed with both a refractive index detector L-2490 and a UV detector.

2.4 Theory of Metabolic Flux Analysis

Calculations of fluxes by metabolite balancing are based on a biochemical pathway model represented in a stoichiometric matrix, whose elements are the coefficients g_{ij}. The rows of the matrix represent the intracellular reactions *j* and the columns represent the metabolites *i* involved in the biochemical reactions. Generally, the dynamics of the metabolite concentrations c_i may be described by equation 1.

$$\frac{dc_i(t)}{dt} = \sum_{j=1}^{k} g_{ij} v_j(t) - \mu(t) c_i \qquad (1)$$

Changes in concentrations of metabolite *i* on a node result from both, the conversion rate ν_j and metabolite dilution due to the change of biomass $\mu(t)$. The last term is generally neglected due to low intracellular concentration of metabolites values against the usually high conversion rates (Stephanopoulos et al., 1998).

The catalytic nature of most of the participating enzymes is subjected to complex regulatory mechanism by metabolite inhibition and activation. The enzyme activities are mainly influenced by the concentrations of metabolites, as well as by the environmental parameters. Assuming steady state conditions leads to a simplification of equation 1:

$$\frac{dc_i(t)}{dt} = 0 = \sum_{j=1}^{k} g_{ij} v_j \qquad (2)$$

Generalization with matrix notation leads to equation 3:

$$G^{\mathrm{T}} \nu = 0 \qquad (3)$$

Splitting of equation 3 into known and unknown rates leads to equation 4, where the indices *m* and *u* refer to the measured and unknown rates, respectively.

$$G^{\mathrm{T}}{}_m \nu_m + G^{\mathrm{T}}{}_u \nu_u = 0 \qquad (4)$$

The unknown rates can be calculated from:

$$\nu_u = -(G_u^{\mathrm{T}})^{\#} G^{\mathrm{T}}{}_m \nu_m \qquad (5)$$

The Moore-Penrose inverse (pseudo inverse) of G_u^{T} is given by:

$$(G_u^{\mathrm{T}})^{\#} = (G_u\, G^{\mathrm{T}}{}_u)^{-1}\, G_{\mathrm{u}} \qquad (6)$$

The metabolic fluxes were estimated using the exchange fluxes of the analytes quantified via HPLC (Section 2.3). Precision in the measurements was taken into account using the diagnosis and gross error analysis proposed by van der Heijden et al. (1994). All calculations were implemented in MatLab (Mathworks Inc., Natick, MA).

2.5 The metabolic model

The metabolic pathways involved in the models for D-glucose or D-xylose consumption are presented in Figure 1. Eukaryotic cells are separated into several compartments. Most of the carbon metabolism takes place in both, the cytosol and the mitochondria. Therefore, to obtain reliable balances for metabolites which do not pass the mitochondrial membrane, the cell has to be divided into compartments, inter alia because the properties of NAD/NADP differ strictly in their physiological role.

Unlike applications with bacterial cells (Delgado and Liao, 1997), the proton acceptors/donors NAD^+/NADH and $NADP^+$/NADPH were considered as different acting cofactors and thus differentiated in the stoichiometric model.

Model for glucose consumption. After the uptake of D-glucose by a high affinity carrier MSTA (van Kuyk et al. 2004), the glucose is phosphorylated by the hexokinase (*HXK*, E.C. 2.7.1.1) to glucose-6-phosphate (G6P).

The further breakdown of G6P into pyruvate (Pyr) and acetyl-CoA (AcCoA) via glycolysis, as well as the pentose-phosphate pathway (PPP), divided into the oxidative and non-oxidative pathway were implemented in the metabolic model. The cell requirements for NADPH and ribose-5-phosphate (R5P), a precursor for nucleotide and L-histidine synthesis, may be supplied by the PPP.

Furthermore, the mannitol-cycle was included in the model considering a two step conversion of D-mannitol by the NAD^+-dependent mannitol-1-

phosphate dehydrogenase (*M1DH*) and the mannitol-1-phosphatase (*MPP*). Fructose-6-phosphate (F6P) is reduced and subsequently dephosphorylated by the mentioned enzymes. In contrast, the catabolism of D-mannitol in ascomycetes is believed to operate in a parallel direction where D-mannitol is oxidized by $NADP^+$-dependent mannitol-2-dehydrogenase (*M2DH*) followed by phosphorylation of D-fructose (Frc) by the ATP-dependent hexokinase (Ruijter et al. 2003).

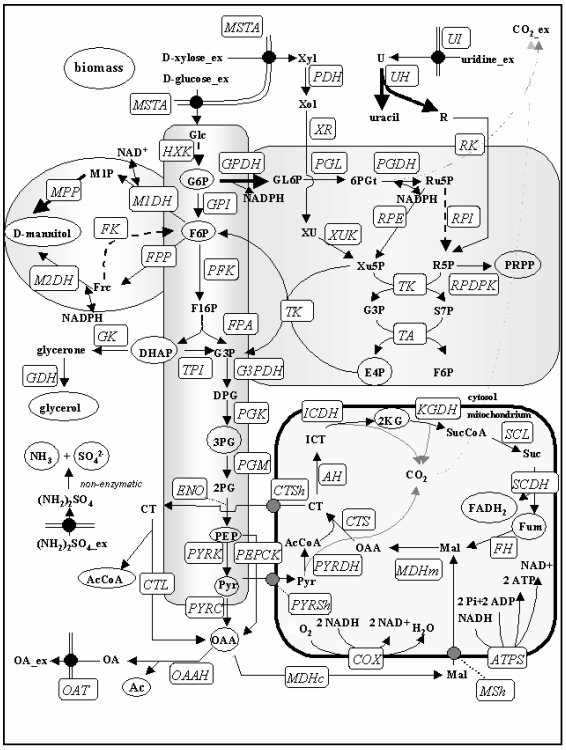

Fig.1: An overview of the main reactions of the metabolic model used for Metabolic Flux Analysis (MFA). Precursor molecules required for growth are shown encircled. Biochemical reactions are catalysed by enzymes, which are shown in rectangles written in cursive capitals. The short cuts of enzyme-names are described in the text.

The carbon dioxide formed by pyruvate dehydrogenase complex (*PYRDH*), which transforms pyruvate (Pyr) into acetyl-CoA (AcCoA), may be used as well by pyruvate carboxylase (*PYRC*) to form oxaloacetate. For modelling purposes, the pyruvate carboxylase activity was assumed to be present in the cytosol (Osmani and Scrutton 1983). The oxaloacetate formed can be reduced to malate (Mal) by the cytosolic malate-dehydrogenase (*MDH*), which is then transported into the mitochondrion by the malate shuttle system. AcCoA is an important precursor for lipid biosynthesis performed in the cytosolic compartment. Hence, citrate is transported via the mitochondrial membrane by the citrate shuttle and subsequently converted by the cytosolic citrate lyase (*CTL*) forming acetyl-CoA and oxaloacetate. Finally, cytosolic oxaloacetate hydrolase (*OAAH*) was assumed to be responsible for the formation of oxalic acid (OA) (Kubicek et al. 1988).

Model for xylose consumption. Most of the enzymatic reactions of the model of D-glucose consumption with the exception of the phosphorylation of glucose to glucose-6-phosphate by the hexokinase, were considered for the D-xylose consumption model. Ensuring the uptake of xylose within the cell, a non-phosphorylating MSTA transport system was assumed, similar to that of the D-glucose.

A successive inter-conversion of the intracellular pool for D-xylose was assumed according to previous works with *A. niger*, *A. nidulans* (Prathumpai et al. 2003) and *Saccharomyces cerevisiae* (Toivari et al. 2004).

After reduction of D-xylose by the polyol dehydrogenase reaction (*PDH*) D-xylitol is either oxidized by the D-xylulose reductase (*XR*) or excreted into the medium via a xylitol transport system. The intracellular pool of D-xylulose is assumed to be further phosphorylated by the ATP-dependent xylulokinase (*XUK*) producing xylulose-5-phosphate (Xu5P). Xu5P serves as a central intermediate entering the non-oxidative part of the pentose phosphate pathway and may be further converted into fructose-6-phosphate (F6P) and glyceraldehyde-3-phosphate (G3P) as a result of the interlinked reaction of the transketolase (*TK*) and transaldolase (*TA*). The intra-mitochondrial constitution of the tricarbon acid cycle (TCA-cycle) as well as the reaction of the GTP-dependent PEP-carboxykinase (*PEPCK*) was considered in both models.

2.6 Requirements for growth

A stoichiometric model for growth was developed including intermediate species existing in the central carbon metabolism (Figure 1). The stoichiometric equations for biomass formation were derived from metabolic models of *A. oryzae* and *A. niger* obtained from Pedersen et al. (1999) and David et al. (2003), respectively. An average protein content of *A. niger* was considered, predicted by the program IdentiCS (Sun and Zeng 2004). This method allows a fast and adequate prediction of protein coding sequences from low coverage genome sequences. The balance equations for biosynthetic pathways for each individual proteinogenic amino acid were taken from David et al. (2003). The biosynthetic pathways for all macromolecules including poly- and monomers have been fractionalized into balance equations containing precursor metabolites:

0.76 3PG + 3.69 AcCoA + 73.24 ATP + 0.078 DHAP + 0.091E4P + 0.41 F6P + 0.078 $FADH_2$ + 1.56 G6P + 0.97 2-KG + 0.21 D-mannitol + 0.65 NAD^+ + 9.64 NAD(P)H + 6.21 NH_3 + 0.3 O_2 + 1.13 OAA + 0.18 PEP + 0.37 PP_i + 0.23 PRPP + 1.84 Pyr + 0.15 SO_4 → 0.151 acetate + 72.5 ADP + 0.61 AMP + 1 gram of dry biomass + 2.04 CO_2 + 3.11 CoA + 0.078 FAD^+ + 0.22 Fum + 0.065 G3P + 0.09 glycerol + 0.65 $NADH^+$ + 9.64 $NAD(P)^+$ + 49.92 P_i (units of coefficients are shown in mmol/g_{DW}).

3. RESULTS AND DISCUSSION

3.1 Flux distribution regarding to Ru5P utilization

The deviations of the flux distribution accounted about 5 to 10 % based on the method of gross error measurement estimation by Heijden et al (1994).
The metabolic models consisted of 54 reactions including 58 intra-cellular metabolites, which after separation in known and unknown rates (Section 2.4) result in over-determined systems for the estimation of unknown fluxes. Additionally, fluxes of 2.2 and 2.5 mmol/g_{dw}/h were measured for O_2 and CO_2, respectively (Example for cultivation with D-xylose at pH 3).
As described in 2.4, after D-xylose uptake the pentose sugar is transformed into Xu5P, which constitutes the entry for the non-oxidative PPP. Additionally, the pool of Xu5P could be provided from Ru5P originating from the oxidative PPP. The latter step is catalyzed by the Ru5P epimerase (*RPE*). Xu5P in combination with R5P are transformed to G3P and seduheptulose-7-phosphate (S7P) by the transketolase reaction. The cellular pool of R5P can be supplied either from Ru5P (from oxidative PPP) by the Ru5P isomerase reaction or from PRPP as a result of a net flux from nucleotides due to RNA- and DNA-degradation. The phosphorylation of D-ribose (R) by the ribose kinase (*RK*) originating from the uridine hydrolysation may occur as well.
In Figure 2, three different cases are demonstrated, which clearly vary in flux distributions (displayed in the rectangles on the arrows). In case a), the metabolic model included the Ru5P epimerase together with Ru5P isomerase. In case b) and c), the Ru5P-isomerase and the epimerase reaction were eliminated from the model, respectively.

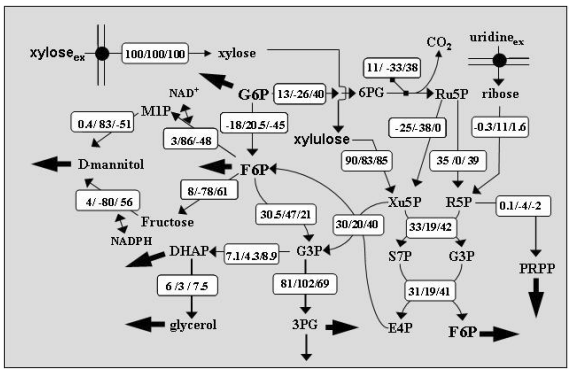

Fig. 2: Flux distribution compared for three different cases: case a), Ru5P-isomerase together with Ru5P-epimerase were considered; case b), without Ru5P-isomerase; case c), without Ru5P-epimerase. Values of flux distribution are listed in the square from left to right for case a), b) and c), respectively. Biomass precursor fluxes are depicted with the bold arrows.

In all cultivations no xylitol was accumulated in the medium. Hence, it can be considered that D-xylose was completely converted into Xu5P by the xylulose kinase. Therefore, this flux was set to 100%. Consequently, all fluxes were calculated normalized in relation to the D-xylose uptake rate.
Considering the case, where the Ru5P-isomerase and epimerase are expressed at the same time, the flux from the non-oxidative PPP into the glycolysis shunt amounts 61% compared to 39% and 81% for case a), b) and c), respectively (the transaldolase as well as the latter step of transketolase produce 2 mol of fructose-6-phosphate entering the glycolysis).
Interestingly, considering the model without isomerase, 38% of the entire incoming D-xylose might be isomerized to Ru5P and, from there, the net flux through the reverse reaction of the oxidative PPP takes place. In this matter, NADPH would be ultimately consumed, which must be generated from another pathway to provide the level of cofactors for biosynthetic power. Therefore, the high flux through the mannitol-cycle may be justified, displayed in Figure 2. The oxidation by the NADP-dependent *M2DH* provides the required amounts of NADPH at the expense of NADH, which is depleted by the *M1DH* forming of mannitol-1-phosphate.
However, the reverse flux of oxidative PPP is thermodynamically feasible but, from the physiological point of view, not possible due to the rapid hydrolysis of the 6-phosphogluconolactone (6PGL) (Beutler and Kuhl 1985). Hence, case b) was not considered for MFA. The results observed for case a) display an apparently “futile” cycle connecting epimerase and isomerase reaction to fill the R5P pool from Xu5P.
In the latter case c), 80% of D-xylose is converted to F6P and G3P, which enter the oxidative PPP to generate NADPH (via the *G6PI*) and the pyruvate synthesis part of glycolysis (via *G3PDH*).
At this point a summary of all observations led to the conclusion, that the Ru5P-epimerase would not be expressed if D-xylose is used as the sole limiting carbon source. Accordingly, all further calculations for cultivation experiments using D-xylose were performed with the model not considering Ru5P-epimerase (*RPE*). Moreover, the flux distribution of case c) was compared based on the assumption, that D-xylose conversion was catalyzed by a two step reaction via the NADP-dependent polyol dehydrogenase (*PDH*) forming xylitol, with a subsequent oxidation forming xylulose by the NAD-dependent xylulose reductase (*XR*) (Eliasson et al 2001). Likewise, another pathway should be considered which could lead to the direct production of xylulose from D-xylose by the D-xylose isomerase (E.C. 5.3.1.5). Although, due to the presence of xylitol in the cells (measured by GC-MS analysis, data not shown) the pathway described above seems to be more probable.
The flux distribution displayed in Figure 3 revealed that the flux of mannitol-cycle can change direction depending on the cofactor properties of xylulose reductase. These results indicated that the demand of NADPH by D-xylitol formation might be balanced in large part by the mannitol-2-dehydrogenase reaction

forming fructose and NADPH. Assuming that the mannitol-1-phosphatase reaction (*MPP*) is irreversible (Schmatz 1997), the model of case d) was considered for further investigations.

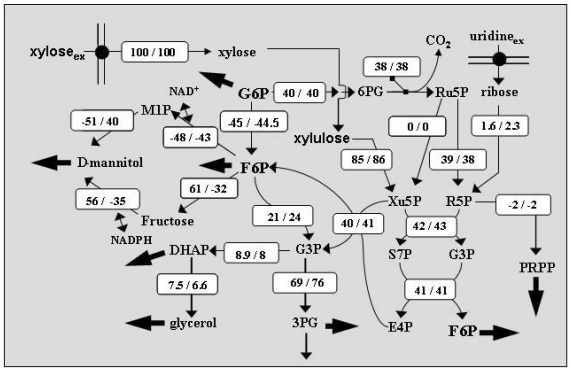

Fig. 3: Case c) including NADP-dependent xylulose-reductase was compared to case d) including a NADH-dependent xylulose reductase. Values of flux distribution are listed in the square from left to right for case c) and d), respectively. Biomass precursor fluxes are depicted with the bold arrows.

3.2 Flux distribution depending on pH and the carbon source

The flux distribution of the central carbon metabolism seems to be rather unaffected regarding to changes of the pH ($3 \leq pH \leq 5.5$) (Figure 4 and 5).

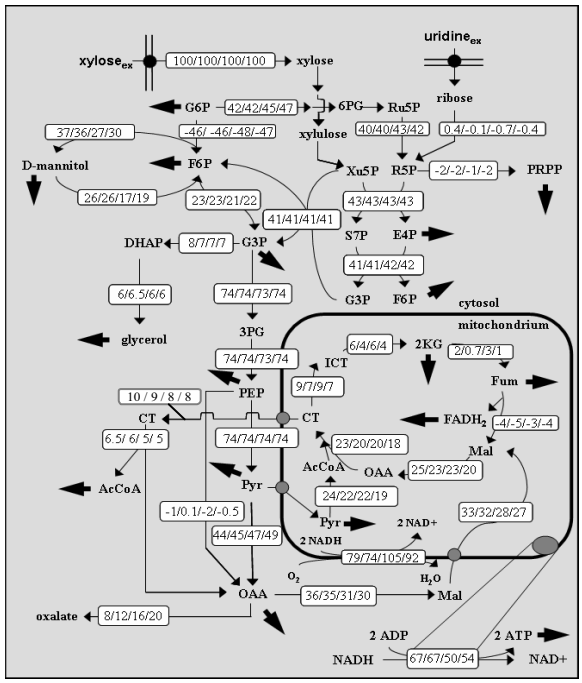

Fig. 4: pH-dependent flux distribution during D-xylose consumption. The flux distributions values were displayed in the squares placed on the reaction path, where the data refer for pH 3, 3.7, 4.7, 5.5 from left to the right, respectively. Biomass precursor fluxes are depicted with the bold arrows.

One exception was observed for the flux through the oxidative PPP with D-glucose consumption, where a maximum (48%) was observed at pH 3.7. This could be correlated with the maximal glucoamylase production yield measured under these conditions (data not shown).

In general, high yields of NADPH with increased flux through the oxidative PPP are correlated with high protein production, which is in a good agreement with the results for *A. oryzae* (Pedersen et al., 1999). A comparison of both models under D-glucose and D-xylose consumption conditions revealed that the flux through the reductive part of the PPP was about 6-fold higher when using D-xylose as the carbon source. Using D-xylose as the sole carbon source redirects the reversible reaction of the glucose-6-phosphate isomerase (*GPI*) to fulfill NADPH requirements for biosynthesis. The additional demand of NADPH for the reduction of xylose to xylitol causes a higher flux through the oxidative part of the PPP and, additionally, an increase of the flux through the mannitol-cycle. In general, the flux through the glycolysis is 1.4-fold higher if D-glucose is used as the sole carbon source. In this case, the flux of the mannitol pool is kept constantly covering the mannitol demand for both, biomass synthesis and oxidative stress prevention (Diano et al. 2006).

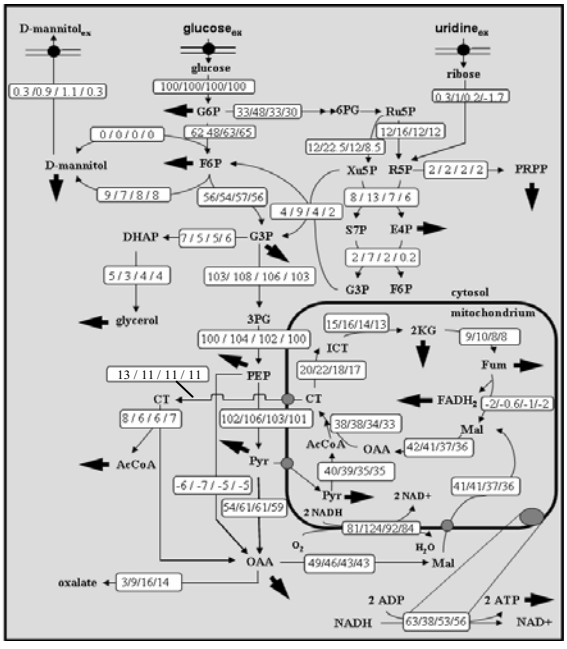

Fig. 5: pH-dependent flux distribution during D-glucose consumption. The flux distributions values were displayed in the squares placed on the reaction path, where the data refer for pH 3, 3.7, 4.7, 5.5 from left to the right, respectively. Biomass precursor fluxes are depicted with the bold arrows.

The flux through the TCA-cycle (e.g. citrate-synthase) is 1.4-fold higher for D-glucose than for D-xylose consumption.

Especially interesting is the increased oxalic acid accumulation with increasing extracellular pH. This is in agreement with data reported by Ruijter et al.

(1999). Accordingly, the model predicts a significant increase in the flux through the *OAAH* reaction with increasing extracellular pH (Figure 6).

The pyruvate branchpoint is an important point of regulation in the metabolism. In the case of D-glucose consumption, more than the half of cytosolic pyruvate is converted into oxaloacetate via the pyruvate carboxylase reaction (*PYRC*), while for D-xylose the amount rises to two-third. This might be caused inter alia by the overproduction of oxalate by the oxalacetase (*OAA*).

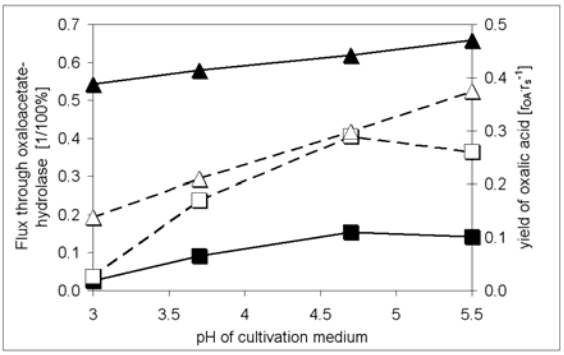

Fig. 6: Yield coefficients of oxalic acid (dashed lines) and flux through the oxaloacetate hydrolase (continuous lines) during D-xylose (triangle) and D-glucose (squares) cultivations.

4. CONCLUSIONS

By means of comparative metabolic flux analysis, it was revealed that the pH of the cultivation medium has practically no appreciable effect on the flux distribution of the central carbon metabolism in *A. niger* AB1.13. An exception was observed for the flux through the oxidative PPP under D-glucose consumption, where a maximum (48%) at pH 3.7 is obtained. This increase in the flux through the oxidative PPP seems to be correlated with high yields of NADPH and, therefore, associated to enhanced protein production.

Acknowledgments: The authors thank the financial support of the German Research Foundation (DFG) for this project.

REFERENCES

Beutler, E. and W. Kuhl (1985). "Limiting role of 6-phosphogluconolactonase in erythrocyte hexose monophosphate pathway metabolism." *J Lab Clin Med* 106(5): 573-577.

David, H., M. Akesson and J. Nielsen (2003). "Reconstruction of the central carbon metabolism of Aspergillus niger." *Eur J Biochem* 270(21): 4243-4253.

Delgado, J. and J. C. Liao (1997). "Inverse flux analysis for reduction of acetate excretion in Escherichia coli." *Biotechnol Prog* 13(4): 361-367.

Diano, A., S. Bekker-Jensen, J. Dynesen and J. Nielsen (2006). "Polyol synthesis in Aspergillus niger: influence of oxygen availability, carbon and nitrogen sources on the metabolism." *Biotechnol Bioeng* 94(5): 899-908.

Eliasson, A. J.-H. S. Hofmeyr, S. Pedler, B. Hahn-Hägerdal (2001). „The xylose reductase/xylitol dehydrogenase/ xylulokinase ratio affects product formation in recombinant xylose-utilising Saccharomyces cerevisiae." *Enzyme and Microbial Technology* 29: 288 – 297.

Kubicek, C. P., G. Schreferl-Kunar, W. Wohrer and M. Rohr (1988). "Evidence for a cytoplasmic pathway of oxalate biosynthesis in Aspergillus niger." *Appl Environ Microbiol* 54(3): 633-637.

Mattern, I. E., J. M. van Noort, P. van den Berg, D. B. Archer, I. N. Roberts and C. A. van den Hondel (1992). "Isolation and characterization of mutants of Aspergillus niger deficient in extracellular proteases." *Mol Gen Genet* 234(2): 332-336.

Osmani, S. A. and M. C. Scrutton (1983). "The sub-cellular localisation of pyruvate carboxylase and of some other enzymes in Aspergillus nidulans." *Eur J Biochem* 133(3): 551-560.

Pedersen, H., M. Carlsen and J. Nielsen (1999). "Identification of enzymes and quantification of metabolic fluxes in the wild type and in a recombinant aspergillus oryzae strain." *Appl Environ Microbiol* 65(1): 11-19.

Prathumpai, W., J. B. Gabelgaard, P. Wanchanthuek, P. J. van de Vondervoort, M. J. de Groot, M. McIntyre and J. Nielsen (2003). "Metabolic control analysis of xylose catabolism in Aspergillus." *Biotechnol Prog* 19(4): 1136-1141.

Ruijter, G. J., M. Bax, H. Patel, S. J. Flitter, P. J. van de Vondervoort, R. P. de Vries, P. A. vanKuyk and J. Visser (2003). "Mannitol is required for stress tolerance in Aspergillus niger conidiospores." *Eukaryot Cell* 2(4): 690-698.

Ruijter, G. J., P. J. van de Vondervoort and J. Visser (1999). "Oxalic acid production by Aspergillus niger: an oxalate-non-producing mutant produces citric acid at pH 5 and in the presence of manganese." *Microbiology* 145 (Pt 9): 2569-76.

Schmatz, D. M. (1997) "The mannitol cycle in Eimeria." *Parasitology*,, 11 (4): 81-89.

Stephanopoulos, G. N., A. A. Aristidou and J. Nielsen (1998). *Metabolic Engineering - Principles and Methodologies*. London, Academic press.

Sun, J. and A. P. Zeng (2004). "IdentiCS--identification of coding sequence and in silico reconstruction of the metabolic network directly from unannotated low-coverage bacterial genome sequence." *BMC Bioinformatics* 5: 112.

Toivari, M. H., L. Salusjarvi, L. Ruohonen and M. Penttila (2004). "Endogenous xylose pathway in Saccharomyces cerevisiae." *Appl Environ Microbiol* 70(6): 3681-3686.

van der Heijden, R. T. J. M., Heijnen, J. J., Hellinga, C., Romein, B. and Luyben, K. Ch. A. M. (1994). "Linear constraint relations in biochemical reactions systems: II. Diagnosis and estimation of gross measurement errors." *Biotechnol Bioeng* 43, 11-20.

van Hartingsveldt, W., I. E. Mattern, C. M. van Zeijl, P. H. Pouwels and C. A. van den Hondel (1987). "Development of a homologous transformation system for Aspergillus niger based on the pyrG gene." *Mol Gen Genet* 206(1): 71-75.

van Kuyk, P. A., J. A. Diderich, A. P. MacCabe, O. Hererro, G. J. Ruijter and J. Visser (2004). "Aspergillus niger mstA encodes a high-affinity sugar/H+ symporter which is regulated in response to extracellular pH." *Biochem J* 379(Pt 2): 375-383.

Vogel, H. (1956). "A convenient growth medium for *Neurospora* (Medium N)." *Microbial Genet. Bull.* 243: 112-119.